

## Accepted Manuscript

Lysosome-targeted two-photon fluorescent probe for detection of hypobromous acid in vitro and in vivo

Chen Ma, Minrui Ma, Yida Zhang, Xinyue Zhu, Lin Zhou, Ran Fang, Xiaoyan Liu, Haixia Zhang



PII: S1386-1425(18)31099-0

DOI: <https://doi.org/10.1016/j.saa.2018.12.029>

Reference: SAA 16658

To appear in: *Spectrochimica Acta Part A: Molecular and Biomolecular Spectroscopy*

Received date: 5 November 2018

Revised date: 6 December 2018

Accepted date: 15 December 2018

Please cite this article as: Chen Ma, Minrui Ma, Yida Zhang, Xinyue Zhu, Lin Zhou, Ran Fang, Xiaoyan Liu, Haixia Zhang , Lysosome-targeted two-photon fluorescent probe for detection of hypobromous acid in vitro and in vivo. Saa (2018), <https://doi.org/10.1016/j.saa.2018.12.029>

This is a PDF file of an unedited manuscript that has been accepted for publication. As a service to our customers we are providing this early version of the manuscript. The manuscript will undergo copyediting, typesetting, and review of the resulting proof before it is published in its final form. Please note that during the production process errors may be discovered which could affect the content, and all legal disclaimers that apply to the journal pertain.

**Lysosome-targeted two-photon fluorescent probe for  
detection of hypobromous acid in vitro and in vivo**

Chen Ma<sup>1</sup>, Minrui Ma<sup>1</sup>, Yida Zhang<sup>1</sup>, Xinyue Zhu<sup>1</sup>, Lin Zhou<sup>1</sup>, Ran Fang<sup>1</sup>, Xiaoyan

Liu<sup>1</sup>, Haixia Zhang<sup>1,\*</sup>

<sup>1</sup>College of Chemistry and Chemical Engineering, Lanzhou University

\*E-mail: zhanghx@lzu.edu.cn

**Abstract**

It is found that hypobromous acid (HOBr) can affect the activity of type IV collagen. Herein, we synthesized a lysosome-targeted fluorescence probe **NA-lyso** based on Suzuki coupling reaction with naphthalimide as a fluorescent group. HOBr can oxidize the amino group and methylthio group, which increased the degree of conjugation of the probe, thereby affecting its optical properties. Accordingly, it can establish a method for the specific detection of HOBr. **NA-lyso** has the properties including fast response, high fluorescence quantum yield ( $\Phi=59.17\%$ ), high selectivity, low cytotoxicity and good membrane-permeability. The probe can locate to lysosome of cells. The potential of the probe as biosensor for HOBr was demonstrated by imaging of exogenous and endogenous HOBr in living cells and in mice. In consequence, **NA-lyso** is expected to be a powerful tool to detect HOBr in complex biosystem and provides a means of exploring physiological functions associated with HOBr in living organisms.

**Keywords:** Fluorescence probe; Hypobromous acid; Two-photon; Lysosome-targeted

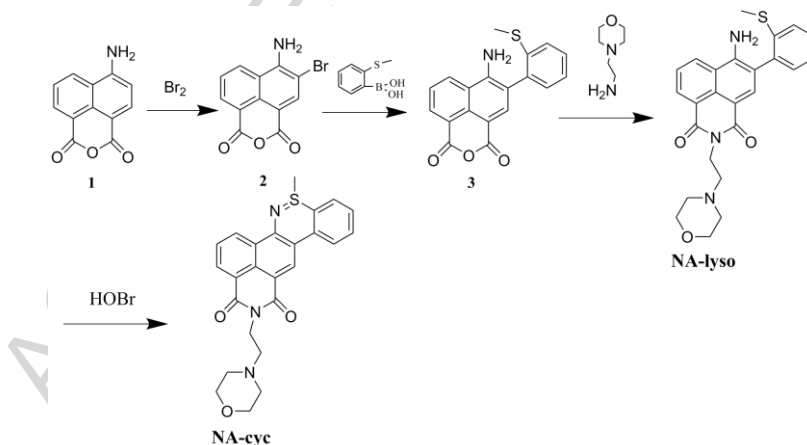
## Introduction

Reactive oxygen species (ROS) are closely related to many biological processes, including cell signaling, cell differentiation, cell growth, and apoptosis [1-3]. Further, they are involved in the pathogenesis of many diseases in organisms [4-6]. HOBr is an important ROS and its chemical properties and structures are very similar with HOCl [7]. There were a lot of detailed research on the role of HOCl in human, for instance, once the body produces an excessive amount of HOCl, it causes various diseases including rheumatoid arthritis and cancer [8-11]. However, research on the physiological effects and detection of HOBr are quite rare [12]. Recent researches have shown that excessive generation and accumulation of HOBr in human body is toxic to organisms and its damaging influences relate to a wide range of diseases, including rheumatoid arthritis [13, 14] and inflammatory tissue damage [15-17].

Hudson and his co-workers reported that HOBr plays an irreplaceable role in the formation of collagen IV in 2014 [18], because HOBr plays a key role in the coupling reaction of hydroxylysine and methionine, while they are components of collagen IV. HOBr is generated from the peroxidation of the bromide anion ( $\text{Br}^-$ ) with hydrogen peroxide, the reaction was catalyzed by a heme peroxidase such as myeloperoxidase (MPO) or eosinophil peroxidase (EPO) [19, 20]. Recently, Tang's group has developed two fluorescence probes for detecting HOBr, one is biphenyl probe (**BPP**), the other is a mitochondria-targeting probe **RhSN-mito**, both of probes are capable of sensitive and selective detection of HOBr [21, 22]. To better understand the

physiological and pathological effects of HOBr at the subcellular level, it is necessary to establish an ultrasensitive method for monitoring the concentration change of HOBr in different organelles. However, there is no probe for detecting endogenous HOBr in lysosomes.

Inspired by the above research, we have developed a lysosome-targeted fluorescent probe **NA-lyso** for the specific detection of HOBr. The synthetic strategy is shown in **Scheme 1**. **NA-lyso** was obtained by a Suzuki cross-coupling reaction. In the presence of HOBr, the amino group on the probe and the methylthio group will undergo a cyclization reaction, and the fluorescence intensity of the cyclic product (**NA-cyc**) weakens sharply. The electron clouds orbital distribution of **NA-lyso** and **NA-cyc** by density functional theory were calculated, verifying that the photoinduced electron transfer (PET) effect results in the fluorescence quenching.



**Scheme 1.** Synthetic route of probe **NA-lyso** and proposed reaction between **NA-lyso** and HOBr

## 2. Experimental Section

## 2.1. Materials and instruments

Liquid bromine, dichloromethane ( $\text{CH}_2\text{Cl}_2$ ), ethanol ( $\text{C}_2\text{H}_5\text{OH}$ ), methanol (MeOH) and toluene were purchased from Tianjin Guangfu Chemical Research Institute (Tianjin, China). 1,1'-bis(diphenylphosphino) ferrocene-palladium (II) chloride dichloromethane complex, 2-methylthiobenzeneboronic acid, silver nitrate ( $\text{AgNO}_3$ ), 4-(2-aminoethyl)morpholine, 6-Dimethyl sulfoxide (d6-DMSO), 4-(2-hydroxyethyl)-1-piperazineethane sulfonic acid (HEPES) were purchased from Energy Chemical Technology (Shanghai, China). N-Acety-L-Cysteine (NAC) was purchased from Sigma Aldrich China (Shanghai, China). DEME medium, MTT (3-(4,5-dimethyl-2-thiazolyl)-2,5-diphenyl-2-H-tetrazolium bromide) was obtained from Sangon Biotech (Shanghai, China). Lyso-Tracker Red, a commercial lysosomal targeting reagent was purchased from Beyotime Biotechnology (Shanghai, China), Ultrapure water was produced from the ALH-6000-U (Aquapro International Company, USA) purification system. All other chemicals were obtained from qualified reagent suppliers with analytical reagent grade.

Fluorescence spectra were measured by a RF-5301pc Fluorescence spectrometer (Shimadzu, Japan) with a Xenon lamp and 1.0-cm quartz cells at the slits of 5/5 nm. Absorption spectra were measured on a UV-visible spectrophotometer (TU-1810, China). The fluorescence quantum yields and two-photon absorption cross section were determined on Fluorescence spectrometer FLSP920 (Edinburgh Instruments Ltd., U.K). High resolution mass spectra (HRMS) were measured using a

APEX II 47e FT-ICR spectrometer with ESI or APCI positive ion mode (Bruker Daltonics, America). NMR spectra were determined by 400 MHz using a JEOL NMR instruments (JEOL, Japan). All  $^1\text{H}$  NMR chemical shifts ( $\delta$ ) are reported relative to residual d6-DMSO ( $\delta = 7.27$  ppm), and all  $^{13}\text{C}$  NMR chemical shifts ( $\delta$ ) are reported relative to d6-DMSO ( $\delta = 40.76$  ppm). MTT Assay were performed using the Spark multimode microplate reader (TECAN, Switzerland). Cell imaging were performed by Two-photon laser confocal microscopy (LSM 510 META, Zeiss, Germany). Mice imaging were performed with an IVIS Spectrum (Carestream Health, Canada)

## 2.2 Synthesis of NA-lyso

The synthesis steps were shown in **Scheme 1**.

Compound **1** was synthesized by previous method in our laboratory [23]. Compound **1** (2 mmol, 0.426 g) was dissolved in 20 mL  $\text{CH}_2\text{Cl}_2$ , and liquid bromine ( $\text{Br}_2$ , 2 mmol, 320 mg) was added. The mixture was kept at  $40^\circ\text{C}$  for 12 h, then the solvent was evaporated under reduced pressure. The crude product was purified by silica gel chromatography ( $\text{CH}_2\text{Cl}_2$ :  $\text{CH}_3\text{OH} = 20:1$ , v / v) to obtain compound **2** with yield 85%.

Compound **2** (0.25 mmol, 72.5 mg), 2-methylthiophenylboronic acid (0.75 mmol, 126 mg), tetrabutylammonium bromide (0.025 mmol, 8.10 mg) and 1,1'-(diphenylphosphine) ferrocene-palladium(II) chloride complex (0.025 mmol, 20.4 mg) were dissolved in 15 mL toluene. Ethanol (8 mL) and  $\text{K}_2\text{CO}_3$  (4 mL, 4 M) were added to the mixture. The resulting solution was kept at  $80^\circ\text{C}$  and stirring under

an Ar gas atmosphere for 24 h and monitored by thin layer chromatography (TLC) discontinuously. After the reaction was completed, the reaction mixture were cooled to room temperature, filtered and concentrated. The crude product was purified by neutral alumina column chromatography ( $\text{CH}_2\text{Cl}_2$ :  $\text{CH}_3\text{OH}$  = 10:1, v / v) to obtain compound **3**, yield 39%.

Continuously, 0.1 mmol (33.5 mg) of compound **3** was dissolved in 10 mL of ethanol, and 0.1 mmol (13.0 mg) of 4-(2-aminoethyl) morpholine was added in the solution. The mixture was refluxing at 78 ° C for 6 h. Then the solvent was removed and the crude product was purified by silica gel chromatography ( $\text{CH}_2\text{Cl}_2$ : $\text{CH}_3\text{OH}$  = 20:1, v / v). **NA-lyso** was obtained with a yield of 60%.

**NA-lyso**:  $^1\text{H}$  NMR (400 MHz, )  $\delta$  = 8.74 (d,  $J$  = 6.7 Hz, 1H), 8.43 (d,  $J$  = 4.9 Hz, 1H), 7.90 (d,  $J$  = 1.9 Hz, 1H), 7.66 (m, 1H), 7.42 (dd,  $J$  = 19.3, 7.4 Hz, 2H), 7.25 (m, 2H), 6.69 (s, 2H), 4.12 (s, 2H), 3.50 (s, 4H), 3.28 (m, 6H), 2.34 (d,  $J$  = 1.9 Hz, 3H).

$^{13}\text{C}$  NMR (100 MHz, )  $\delta$  =164.27(s), 163.42(s), 149.58(s), 139.24(s), 135.95(s), 135.76(s), 133.11(s), 131.46(s), 131.05(s), 130.37(s), 129.69(s), 129.54(s), 125.78(s), 125.70(s), 125.03(s), 124.76(s), 122.30(s), 120.52(s), 119.18(s), 108.27(s), 102.93(s), 66.38(s), 56.63(s), 54.09(s), 36.66(s), 14.87(s). HRMS (ESI, m/z) Calcd for  $\text{C}_{25}\text{H}_{26}\text{N}_3\text{O}_3\text{S}$   $[\text{M}+\text{H}]^+$ : 448.1689, found: 448.1690.

### 2.3 Preparation of HOBr and $^-\text{OBr}$

*Preparation of HOBr.* Liquid bromine (100  $\mu\text{L}$ ) was dissolved in ultrapure water (15 mL), then titrated with 0.2 M  $\text{AgNO}_3$  solution in an ice bath until the brown color

disappear. Then the solution was filtered with 0.22  $\mu\text{M}$  filter membrane.

Lambert–Beer’s law was used to calculate the concentration of HOBr ( $\epsilon_{260} = 160 \text{ L mol}^{-1} \text{ cm}^{-1}$ [21]).

*Preparation of  $\cdot\text{OBr}$ .* Sodium hydroxide (1.20 g) was dissolved in 10 mL ultrapure water (10 mL), and 0.768 mL  $\text{Br}_2$  was added to the solution dropwise in an ice bath. The concentration of  $\cdot\text{OBr}$  was calculated ( $\epsilon_{329} = 332 \text{ L mol}^{-1} \text{ cm}^{-1}$ [21])

2.4 Determination of fluorescence quantum yield ( $\Phi$ ) and two-photon absorption cross section (TPACS)

Femtosecond (fs) fluorescence measurement technology was used to determine fluorescence quantum yield of **NA-lyso** ( $1.0 \times 10^{-6} \text{ M}$ , HEPES 7.4) with fluorescein ( $\Phi\%$ : 92% ,  $2.4 \times 10^{-5} \text{ M}$  in NaOH solution, pH=11) as the reference. The fluorescence quantum yields are calculated by the equation (1). Eight wavelengths (760, 780, 800, 820, 840, 860, 880 and 900 nm) were utilized as excitation wavelength to measure the two photon absorption cross section value of **NA-lyso**, and the value was calculated with the equation (2).

$$\Phi_x = \Phi_s (A_s F_x / A_x F_s) (n_x / n_s)^2 \quad (1)$$

$$\delta_x = \delta_s \frac{\Phi_s C_s n_s S_s}{\Phi_x C_x n_x S_x} \quad (2)$$

Where,  $\Phi$  is the fluorescence quantum yield, A is the absorbance at the excitation wavelength, F is the area under the corrected emission curve, n is the refractive index of solvent,  $\delta$  is value of the two photon section, C is the concentration, and the S shows the fluorescence emission intensity of the two photon. Subscript s and x

corresponding to the reference and the samples respectively.

## 2.5 Spectral experiments

The stock solution of **NA-lyso** (1.0 mM) was prepared in DMSO. Samples were prepared by placing 20.0  $\mu\text{L}$  of probe (1.0 mM) and an appropriate aliquot of each analyte solution into a 2.0 mL centrifugal tube, and the volume was fixed finally to 2.0 mL with HEPES (10 mM, pH 7.4 ). The resulting solution were shaken by vortex at room temperature, fluorescence and UV spectra were recorded. Fluorescence spectra were recorded at 430/540 nm with the slits 5/5 nm.

## 2.6 Cytotoxicity Assay

Cell viability was measured by MTT method [24]. Hela cells were seeded in 96-well plates with 200  $\mu\text{L}$  per well at a concentration of  $1.0 \times 10^4$  cells/well, and different concentrations of **NA-lyso** (10, 20, 30, 40, 50 and 100  $\mu\text{M}$ ) were added, then the cells were incubated for 24 h. The control group were treated only with PBS buffer at pH = 7.4 and incubated under the same conditions. After incubation for 24 h, the medium were removed from each well, and 100  $\mu\text{L}$  of MTT solution (0.5 mg/mL, DEME) was added to each well. The cells further were incubated for 4 h at 37  $^{\circ}\text{C}$ . After that, the medium was removed carefully and the formazan solid was dissolved by adding 100  $\mu\text{L}$  of DMSO. The UV absorbance of each well plate was read using a microplate reader. The cell survival ratio (VR) =  $A/A_0 \times 100\%$ . Here, A is the absorbance of the experimental cells, and  $A_0$  is the absorbance of the control cells. Each test was repeated five times, and the data are shown as the mean  $\pm$  SD.

## 2.7 Imaging of HOBr in HeLa cells

HeLa cells were plated on 6-well plates and allowed to adhere for 24 h, and the cells were divided into five parallel groups. The first group was as a blank control and the other groups were incubated with **NA-lyso** (20  $\mu\text{M}$ ). The second group was as a reagent blank control. All the cells were incubated for 30 min at 37°C. The third was added  $\text{Br}^-$  (20  $\mu\text{M}$ ); the fourth was added HOBr (20  $\mu\text{M}$ ); the fifth group was added  $\text{Br}^-$  (20  $\mu\text{M}$ ) and NAC (20  $\mu\text{M}$ ). All groups containing 0.1% DMSO as a cosolvent and then every parallel was cultivated for another 30 min. Before imaging, the cells were washed with PBS (pH = 7.4) buffer for three times.

For colocalization experiments, one group of cells was incubated with 20  $\mu\text{M}$  Lyso-Tracker Red for 30 min, another group were incubated with 20  $\mu\text{M}$  **NA-lyso** for 30 min. Before the imaging experiment, all groups of cells were rinsed with PBS for three times, and the fluorescence images were acquired through a two-photon laser confocal microscopy with excitation wavelength as 800 nm, collecting green channel of 520-560 nm (LSM 510 META , Zessi , Germany).

## 2.8 Imaging of HOBr in Kunming Mice

Kunming mice (KM, female, 5-6 weeks old) were obtained from Gansu University of Chinese Medicine. All animal experiments were performed in accordance with the guidelines issued by The Ethical Committee of Gansu University of Chinese Medicine.

Kunming mice were divided into four groups, the first group was as control

group; the second group was given an Intraperitoneal (i.p.) injection of saline (200  $\mu\text{L}$ ) containing 0.1% DMSO; the third group was given an i.p. injection of 200  $\mu\text{L}$  **NA-lyso**; and the last group was given an i.p. injection of NaBr (200  $\mu\text{L}$ , 100  $\mu\text{M}$ ), after 30 min, given i.p. injection of 200  $\mu\text{L}$  **NA-lyso**. The **NA-lyso** was prepared in 100  $\mu\text{M}$  in saline containing 0.1% DMSO as cosolvent. After the i.p. injection, each group was kept for 30 min and then for image.

The mice were imaged as quadruplets, one from each group using an IVIS Spectrum (Carestream Health, Canada) in fluorescence mode equipped with 420 and 560 nm filters for excitation and emission, respectively. Photographs were taken using a fixed exposure time.

### 3. Results and discussion

#### 3.1 Synthesis of probe **NA-lyso**

The probe was successfully synthesized based on Suzuki coupling reaction according to **Scheme 1** with naphthalimide as a fluorescent group, and the structure of **NA-lyso** was characterized by  $^1\text{H}$  NMR,  $^{13}\text{C}$  NMR and HRMS spectra (see **Figure S5-S7** in Supporting Information).

#### 3.2 Spectroscopic property and optical response to HOBr

The fluorescence quantum yield of **NA-lyso** is 59.17% and its two-photon cross section under different wavelength excitations were obtained and calculated using Equation 2. The calculative result is shown in **Figure S8**. The largest two-photon

cross section is obtained at 800 nm excitation, which is 88.8 GM.

**NA-lyso** has a strong absorption peak at 437 nm (**Figure 1a**), upon the addition of HOBr, the absorption of the probe is red-shifted to 451 nm and the fluorescence intensity at 540 nm is significantly weakened (**Figure 1b**). This phenomena can be attributed to the formation of nitrogen-sulfur double bond by the amino group and methylthio group in the probe under the action of HOBr (**Scheme 1**). This conjecture was verified by HRMS, as illustrated in **Figure 2**, the characteristic peak of the product **NA-cyc** (the product of **NA-lyso** and HOBr) appears in the HRMS spectrum.

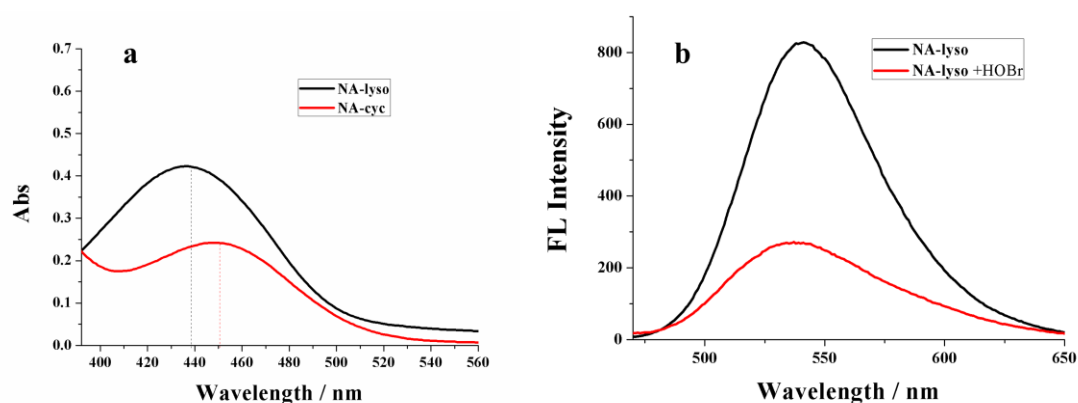


**Figure 1.** UV-Vis (a) and Fluorescence emission spectra (b) of **NA-lyso** (black) and the product **NA-cyc** (red). The concentration of **NA-lyso** and HOBr were 10  $\mu\text{M}$  and 40  $\mu\text{M}$  respectively.  $\lambda_{\text{ex}} = 430 \text{ nm}$ .

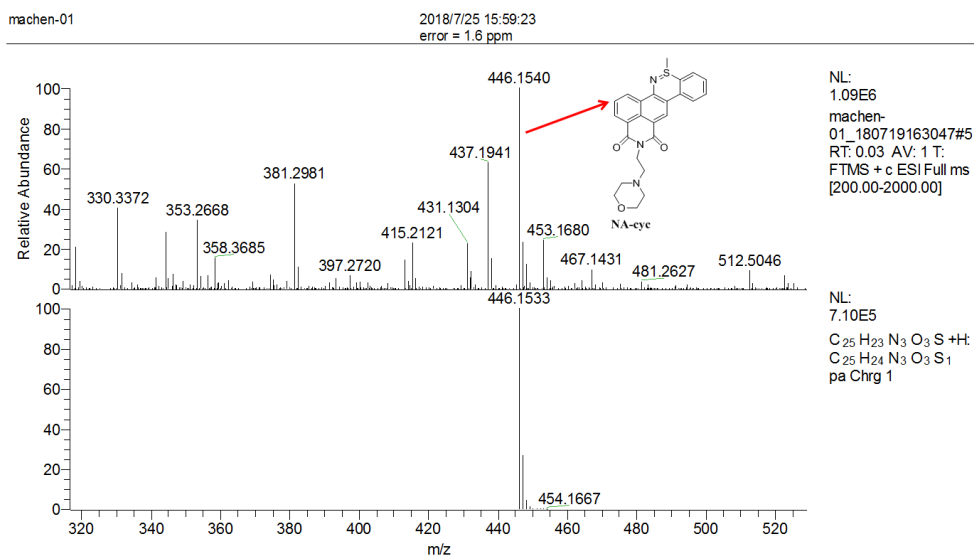


**Figure 2.** The HRMS of NA-cyc

### 3.3 Study on the luminescence mechanism of probe

To illustrate the fluorescence "on-off" phenomenon, we calculated the electron cloud orbital distribution of the probe **NA-lyso** and the reaction product **NA-cyc** through the density functional theory by the Gaussian 09 software [DFT at the b3lyp/6-311g (d,p) level]. The calculated result is shown in **Figure S9**, we can get the information that the electron clouds in the LUMO and HUMO orbits of **NA-lyso** are both distributed on the naphthalimide ring, thus there is no photoinduced electron transfer (PET) effect. For **NA-cyc**, the electron cloud density in LUMO is mainly distributed on the naphthalimide ring, however, the electron cloud in HUMO is mainly distributed on 4-(2-aminoethyl) morpholine, thus cause PET, which leads to fluorescence quenching of **NA-cyc**. In addition, the energy differential of **NA-lyso** and **NA-cyc** are 0.3282 and 0.3035 eV respectively, which are basically consistent. It

is also confirmed that the PET effect occurs in **NA-cyc**, leading to the fluorescence quenching.

### 3.4 Optimization of measurement conditions

First, the fluorescent intensities of **NA-lyso** and **NA-cyc** in HEPES buffers with different pH ranging from 3.0 to 10 were recorded (**Figure 3a**). After HOBr was added, fluorescence intensity were receded dramatically. When the pH is less than 8.0, the fluorescence of **NA-lyso** and **NA-cyc** are relatively stable, but when the pH is larger than 8.0, the degree of fluorescence response is reduced. The reason is that  $\text{O}^-$  is the main form when the pH is larger than 8 (pKa of HOBr is 8.8 at 25 °C [12]), and the real concentration of HOBr in the system was reduced, which weakened the response of **NA-lyso** to HOBr.

The response of **NA-lyso** to HOBr is so fast that the fluorescence intensity immediately weakens when added HOBr to the system and remains stable for a long time. The fluorescence intensities of **NA-lyso** and **NA-cyc** show hardly changes within 60 min (**Figure 3b**), which indicate the probe has good resistance to photobleaching and **NA-cyc** could remain stable.

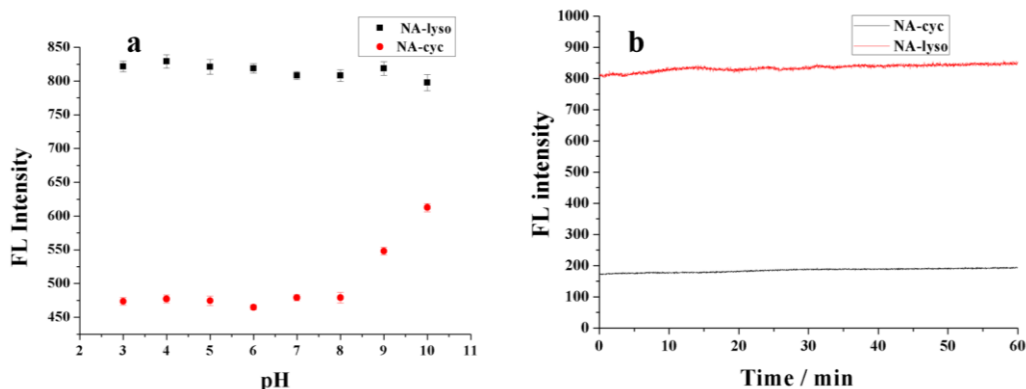


**Figure 3.** Effect of pH (a) and time (b) on the response of the reaction system

The concentration of **NA-lyso** and HOBr were 10  $\mu\text{M}$  and 40  $\mu\text{M}$  respectively.

$$\lambda_{\text{ex}} = 430 \text{ nm}; \lambda_{\text{em}} = 540 \text{ nm.}$$

### 3.5 Fluorescence responses of **NA-lyso** to HOBr

The fluorescence responses of **NA-lyso** to HOBr with different concentration (0-40  $\mu\text{M}$ ) were investigated in HEPES 7.4 (10 mM) at room temperature. **Figure 4a** shows that the fluorescence intensity of the reaction product decreased with a dose-dependent manner over a concentration range of HOBr. As depicted in **Figure 4b**, there is a good linearity between  $(F_0-F)/F_0$  and the concentration of HOBr in the range of 0 to 35  $\mu\text{M}$ , while  $F_0$  and  $F$  indicate the fluorescence intensity in the absence and presence of HOBr respectively. The regression equation is  $(F_0-F)/F_0 = 0.0179[C_{\text{HOBr}}(\mu\text{M})] - 0.0333$ , with a linear coefficient of 0.990. The limit of detection ( $3S/\sigma$ ) was determined to be as low as 33.5 nM, which makes **NA-lyso** practicable for monitoring endogenous HOBr.

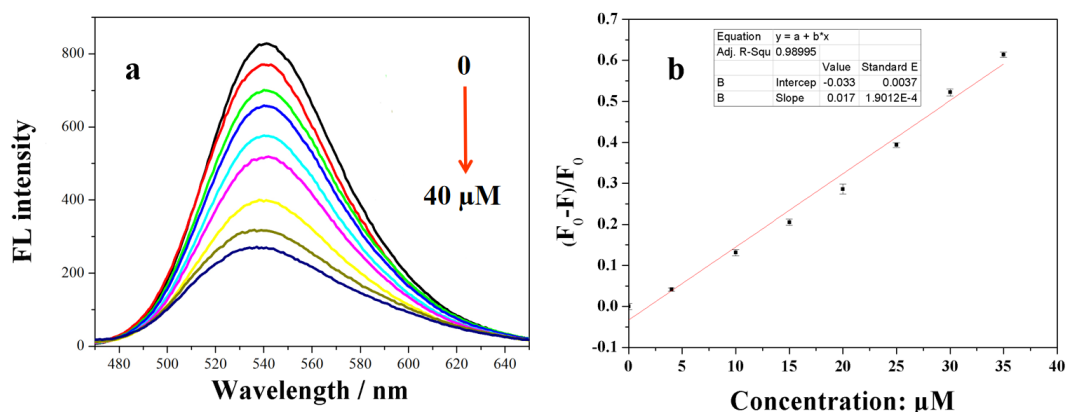


**Figure 4.** a) Fluorescence intensities of **NA-lyso** (10  $\mu\text{M}$ ) treated with increasing concentrations of HOBr in HEPES (10 mM, pH 7.4, 0.1% DMSO as a cosolvent). Silt width: 5/5 nm,  $\lambda_{\text{ex}} = 430$  nm; b) Linear correlation between  $(F_0-F)/F_0$  and concentrations of HOBr in the range of 0-35  $\mu\text{M}$ .

### 3.6 Specificity of **NA-lyso** for detecting HOBr

To inspect whether **NA-lyso** could specifically monitor HOBr in the complicated intracellular environment, we tested its ability to discriminate between HOBr and various bioanalytes, such as competing ROS and RNS (**Figure 5a**). Only HOBr can reduce the fluorescence intensity of **NA-lyso**, correspondingly,  $(F_0-F)/F_0$  has a larger value. When HOBr coexist with other ROS and RNS (**Figure 5b**),  $(F_0-F)/F_0$  shows almost no change, which indicated **NA-lyso** could detect HOBr with excellent selectivity and satisfactory anti-interference performance in complicated system. Moreover, the probe do not respond with  $\text{Br}^-$  and  $^-\text{OBr}$ , and they have no effect on the response of probe to HOBr as well.

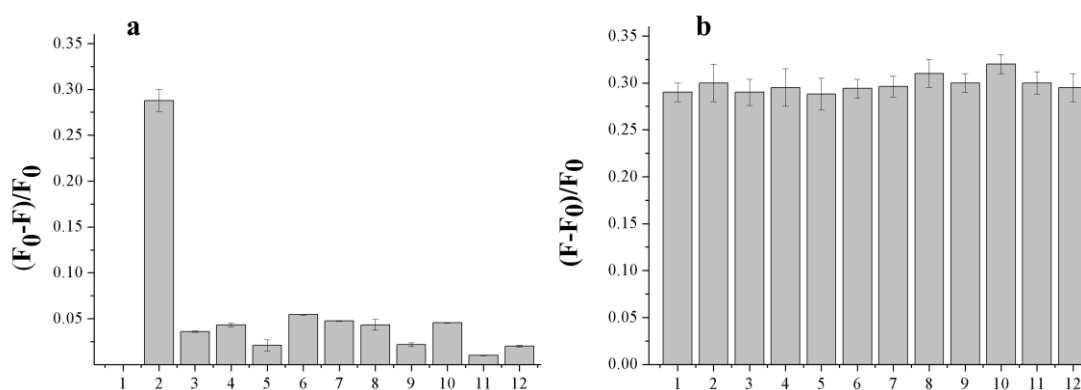


**Figure 5.** The fluorescence responses of **NA-lyso** (10  $\mu\text{M}$ ) in the presence of various analytes. 1:Blank, 2: HOBr, 3:  $\cdot\text{OH}$ , 4:  $\text{ONOO}^-$ , 5:  $t\text{-BuO}\cdot$ , 6:  $\text{O}_2^-$ , 7:  $\text{H}_2\text{O}_2$ , 8: NO, 9: HOCl, 10:  $t\text{-BuOOH}$ , 11:  $\text{Br}^-$ , 12:  $\text{OBr}^-$ . (a) Fluorescence responses of **NA-lyso** with various analytes; (b) fluorescence responses of **NA-lyso** towards HOBr plus the corresponding analytes. The concentration of all analytes were 10  $\mu\text{M}$ .  $\lambda_{\text{ex}}=430$  nm,  $\lambda_{\text{em}}=540$  nm.

### 3.7 Cell imaging of probe **NA-lyso**

Inspired by outstanding optical property ( $\Phi=59.17\%$ , TPACS=88.8 GM) of **NA-lyso** and its sensitivity towards HOBr, we proceed to investigate the potential application of the probe in fluorescence imaging in cells. Firstly, an MTT assay was performed in Hela cells (**Figure S10**). When the concentration of **NA-lyso** were 100  $\mu\text{M}$ , there was no significant reduction in cell viability, indicating the probe had favorable biocompatibility. Subsequently, the colocalization experiment was conducted by costaining Hela cells with Lyso-Tracker Red (a typical commercially available lysosomal tracker) and **NA-lyso** (**Figure 6**). The fluorescence of **NA-lyso** from the costained cells overlaid well with that from Lyso-Tracker Red (**Figure 6c**),

and the Pearson's coefficient is so high as 0.95 (calculated by Image J), which demonstrates **NA-lyso** can locate to the lysosome of Hela cells.

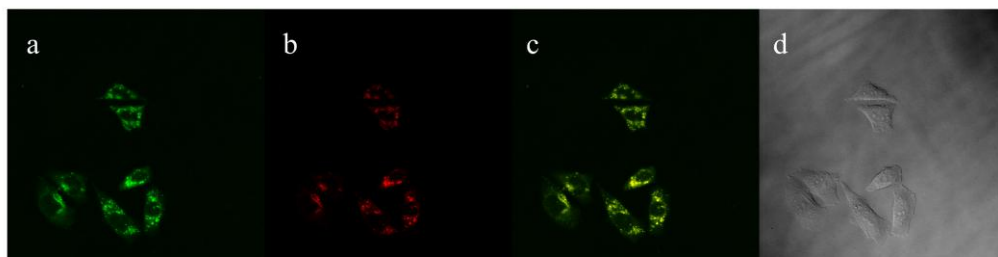


**Figure 6.** Fluorescence images of lysosome in HeLa cells. HeLa cells were incubated with **NA-lyso** (**a**, 20  $\mu\text{M}$ ,  $\lambda_{\text{ex}} = 800 \text{ nm}$ ,  $\lambda_{\text{em}} = 520\text{--}560 \text{ nm}$ ) and Lyso-Tracker Red (**b**, 10  $\mu\text{M}$ ,  $\lambda_{\text{ex}} = 600 \text{ nm}$ ,  $\lambda_{\text{em}} = 620\text{--}700 \text{ nm}$ ) respectively. (**c**) merged image of (**a**) and (**b**); (**d**) bright field image.

Next, we investigated whether the probe can detect HOBr in cells under physiological conditions. As shown in **Figure 7**, a strong fluorescence signal was observed in HeLa cells which were treated only with **NA-lyso** (**Figure 7b**), which meant the probe can easily enter into the cells. When the cells were stimulated with NaBr or HOBr, the fluorescence intensities of cells were declined sharply (**Figure 7c** or **7d**). The reason of **NA-lyso** responding to  $\text{Br}^-$  is that  $\text{Br}^-$  changed to HOBr in cells under the existence of EPO or MPO, but not all the  $\text{Br}^-$  can change to HOBr in a short time. So the fluorescence intensity in **Figure 7c** was less darker than in **Figure 7d**. Additionally, when the cells were treated with  $\text{Br}^-$  and the scavenger (NAC) of HOBr in sequence, the fluorescence intensity of the cells became brighter owing to the decreasing of HOBr concentration (**Figure 7e**).

Through the image J software, we compared the fluorescence intensity from **Figure 7a** to **7e**, the fluorescence intensity from **Figure 7e** is slightly stronger than that from **Figure 7b**, the reason is that NAC not only reacted with exogenous HOBr, but also with endogenous HOBr from the cells.

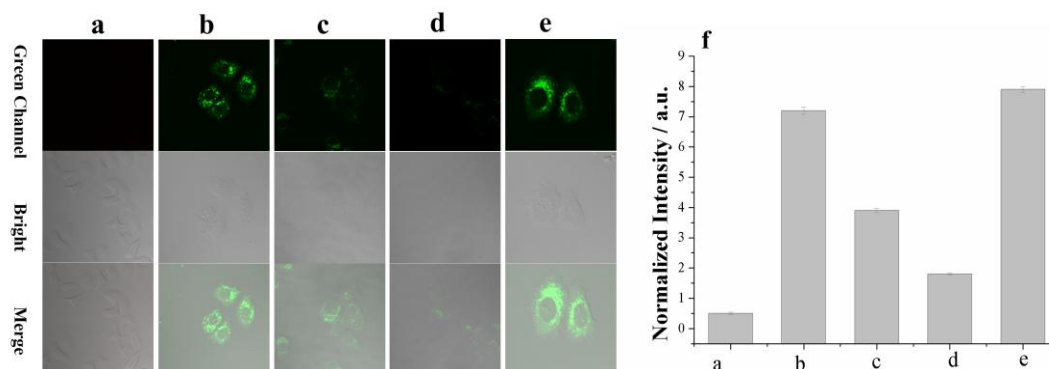


**Figure 7.** Fluorescence images of HeLa cells. **(a)** blank cells; **(b-e)** cells were incubated with **NA-lyso** (20  $\mu$ M) for 30 min **(b)** and subsequently incubated for 30 min with 20  $\mu$ M NaBr **(c)** or 20  $\mu$ M HOBr **(d)** or 20  $\mu$ M NaBr plus 20  $\mu$ M NAC **(e)**. **(f)** Normalized fluorescence intensity of cells in panels **(a)** to **(e)**.  $\lambda_{\text{ex}} = 800$  nm,  $\lambda_{\text{em}} = 520-560$  nm, scale bar = 25  $\mu$ m.

### 3.8 Fluorescence imaging of HOBr in mice

The mice that were given an intraperitoneal (i.p.) injection of **NA-lyso** have very strong fluorescence (**Figure 8c**). The mice were i.p. injection with  $\text{Br}^-$  and **NA-lyso** (20  $\mu$ M) (**Figure 8d**), in which the fluorescence intensity significantly decreased, indicating that **NA-lyso** could visualize endogenous HOBr in living mice. These fluorescence images prove that HOBr can be generated from  $\text{Br}^-$  in mice and

confirm **NA-lyso** is a potential tool for detecting HOBr in vivo.

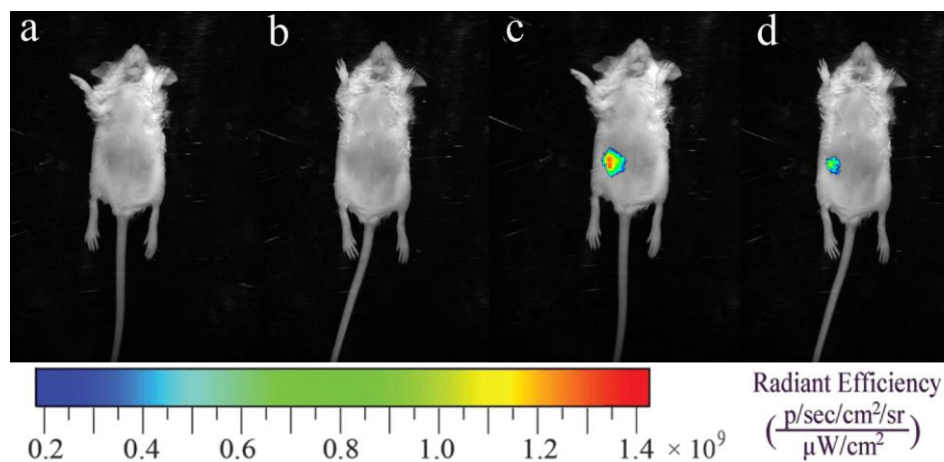


**Figure 8.** Fluorescence imaging of HOBr in living mice. **a)** Mice without any treatment, **b)** mice with i.p. injection of saline solution, **c)** mice with i.p. injection of **NA-lyso** (20  $\mu\text{M}$ ) for 30 min, **d)** mice with i.p. injection of  $\text{Br}^-$  (100  $\mu\text{M}$ ) for 30 min and then with **NA-lyso** (20  $\mu\text{M}$ ) for another 30 min.

The properties of probe **NA-lyso** were compared with the existing probes for HOBr and the result is shown in **Table S1** in Supporting Information. The probe can target to lysosome and is capable of detection of HOBr, moreover, it can be also used for cells and mice imaging owing to the longer excitation wavelength.

## Conclusion

In summary, we developed a high quantum yield lysosome-targeting two-photo fluorescence probe **NA-lyso** for specific monitoring of HOBr. The probe has low limit of detection (33.5 nM) for HOBr with good sensitivity and selectivity. This

probe is capable of targeting to lysosome and monitoring the level of exogenous and endogenous HOBr in Hela cells under excitation of two-photon wavelength. Moreover, the probe can also be used to image HOBr in mice. Overall, **NA-lyso** is an ideal tool for the further research of detection of HOBr and has potential application in further exploration of physiological and pathological roles of HOBr in lysosome. However, it should continue to develop the new probe for accurate quantification of HOBr in cells.

#### **Acknowledgement**

This research was financially supported by the National Natural Science Foundation of China (No. 21575055).

**References**

- [1] X. Chen, X. Tian, I. Shin, J. Yoon. Fluorescent and luminescent probes for detection of reactive oxygen and nitrogen species. *Chem. Soc. Rev.* 40 (2011) 4783-4804.
- [2] C. Nathan. Specificity of a third kind: reactive oxygen and nitrogen intermediates in cell signaling. *J. Clin. Invest.* 111 (2003) 769.
- [3] P. F. Bove, A.V.D. Vliet. Nitric oxide and reactive nitrogen species in airway epithelial signaling and inflammation. *Free Radical Bio.Medi.* 41 (2006) 515-527.
- [4] S. K. Ko, X. Chen, J. Yoon, I. Shin. Zebrafish as a good vertebrate model for molecular imaging using fluorescent probes. *Chem. Soc. Rev.* 40 (2011) 2120-2130.
- [5] X. Q. Chen, Y. Zhou, X. J. Peng, J. Y. Yoon. Fluorescent and colorimetric probes for detection of thiols. *Chem. Soc. Rev.* 39 (2010) 2120 - 2135.
- [6] K. Kikuchi. Design, synthesis and biological application of chemical probes for bio-imaging. *Chem. Soc. Rev.* 39 (2010) 2048-2053.
- [7] D. I. P. And, M. J. Davies. Kinetic Analysis of the Reactions of Hypobromous Acid with Protein Components: Implications for Cellular Damage and Use of 3-Bromotyrosine as a Marker of Oxidative Stress. *Biochemistry.* 43 (2004) 4799-4809.
- [8] W. A. Rutala, D. J. Weber. Uses of inorganic hypochlorite (bleach) in health-care Facilities. *Clin. Microbiol. Rev.* 10 (1997) 597 - 610.
- [9] Y. W. Yap, M. Whiteman, B. H. Bay, Y. Li, F.-S. Sheu, R. Z. Qi, C. H. Tan, N. S.

Cheung, Hypochlorous acid induces apoptosis of cultured cortical neurons through activation of calpains and rupture of lysosomes, *J. Neurochem.* 98 (2006) 1597-1609.

[10] B. B. Deng, M. G Ren, X. Q. Kong, K. Zhou, W. Y. Lin. Development of an enhanced turn-on fluorescent HOCl probe with a large Stokes shift and its use for imaging HOCl in cells and zebrafish. *Sensors and Actuators B* 255 (2018) 963 – 969.

[11] X. Q. Chen, F. Wang, J. Y. Hyun, T. W. Wei, J. Qiang, X. T. Ren, I. Shin, J. Yoon, Recent progress in the development of fluorescent, luminescent and colorimetric probes for detection of reactive oxygen and nitrogen species, *Chem. Soc. Rev.* 45 (2016) 2976 – 3016.

[12] F .Yu, P. Song, P. Li, B. Wang, K. Han. Development of reversible fluorescence probes based on redox oxoammonium cation for hypobromous acid detection in living cells. *Chem. Commun.* 48 (2012) 7735-7737.

[13] J. J. Hu, N. K. Wong, S. Ye, X Chen, M. Y. Lu, A. Q. Zhao, Y. Guo, A.C. Ma, A.Y. Leung, J .Shen, D.Yang. Fluorescent Probe HKSOX-1 for Imaging and Detection of Endogenous Superoxide in Live Cells and In Vivo. *J. Am. Chem. Soc.*137 (2015) 6837-6843.

[14] K. Giannakis, T. Andronikos. Membrane automata for modeling biomolecular processes. *Nat. Comput.* 16 (2017) 1-13.

[15] A. E. Lane, J. T. Tan, C. L. Hawkins, A. K. Heather, M. J. Davies. The myeloperoxidase-derived oxidant HOSCN inhibits protein tyrosine phosphatases and modulates cell signalling via the mitogen-activated protein kinase (MAPK) pathway

in macrophages. *Free Radical Bio. Medi.* 49 (2010) 161-169.

[16] M. J. Ceko, K. Hummitzsch, N. Hatzirodos, W. Bonner, S. A. James, J. K. Kirby, R. J. Rodgers, H. H. Harris. Distribution and speciation of bromine in mammalian tissue and fluids by X-ray fluorescence imaging and X-ray absorption spectroscopy. *Metallomics.* 7 (2015) 756-765.

[17] J. C. van Dalen, W. M. Whitehouse, C. C. Winterbourn, J. A. Kettle. Thiocyanate and chloride as competing substrates for myeloperoxidase. *Biochem. J.* 327(1997) 487-492.

[18] A. S. McCall, C. F. Cummings, G. Bhave, R. Vanacore, B. G. Hudson. Bromine is an essential trace element for assembly of collagen IV scaffolds in tissue development and architecture. *Cell.* 157 (2014) 1380-1392.

[19] W. Wu, Y. Chen, A. D' Avignon, S. L. Hazen. 3-Bromotyrosine and 3,5-dibromotyrosine are major products of protein oxidation by eosinophil peroxidase: potential markers for eosinophil-dependent tissue injury in vivo. *Biochemistry.* 38 (1999) 3538-3548.

[20] B.S. Wang, P. Li, F.B. Yu, J.S. Chen, Z.J. Qu and K.L. Han. A near-infrared reversible and ratiometric fluorescent probe based on Se-BODIPY for the redox cycle mediated by hypobromous acid and hydrogen sulfide in living cells *Chem. Commun.* 49 (2013) 5790—5792.

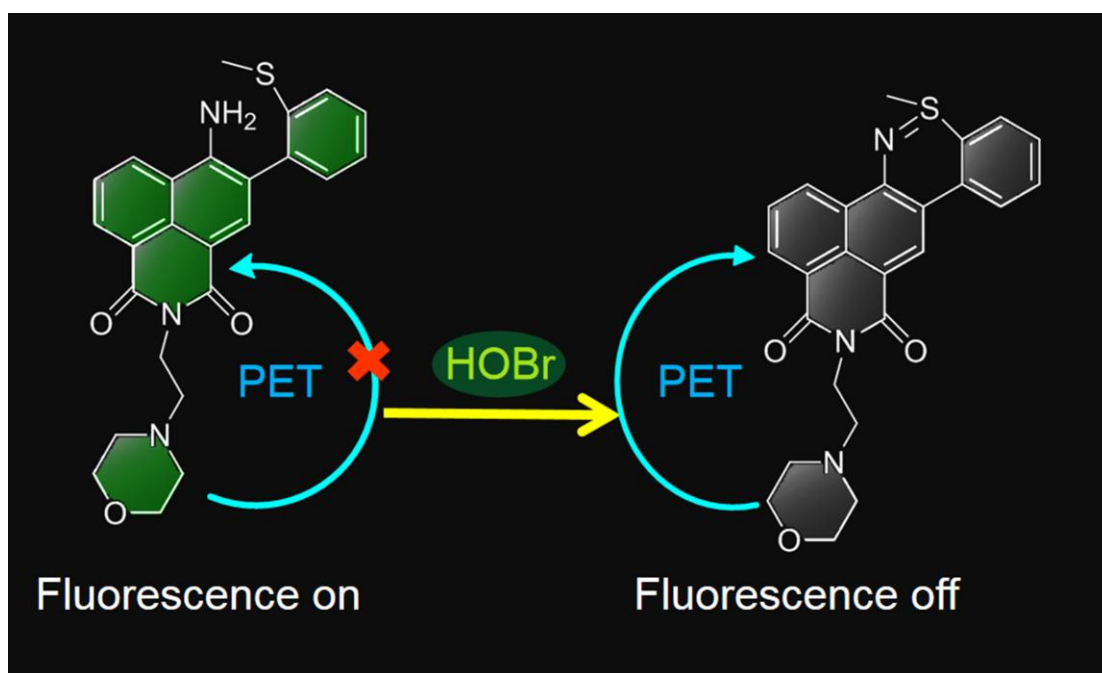
[21] K. H. Xu, D. R. Luan, X. T. Wang, B. Hu, X. J. Liu, F. P. Kong, B. Tang. An Ultrasensitive Cyclization-Based Fluorescent Probe for Imaging Native HOBr in Live

Cells and Zebrafish. *Angew. Chem. Int. Ed.* 55 (2016) 1-5.

[22] X.J Liu, A.S. Zheng, D.R. Luan, X.T. Wang, F.P. Kong, L.L.Tong, K.H. Xu, B. Tang. High-Quantum-Yield Mitochondria-Targeting Near-Infrared Fluorescent Probe for Imaging Native Hypobromous Acid in Living Cells and in Vivo. *Anal. Chem.* 89(2017) 1787–1792.

[23] C. Ma , F. Y. Zhang , Y. Y. Wang, X. Y. Zhu, X. Y. Liu, C. Y. Zhao, H. X. Zhang. Synthesis and application of ratio fluorescence probe for chloride. *Anal. Bioanal. Chem.* 410 (2018) 6507-6516.

[24] J. Kang, F. J. Huo, Y. B. Zhang , J. B. Chao, T. E. Glass, C.X. Yin. A novel near-infrared ratiometric fluorescent probe for cyanide and its bioimaging applications. *Spectrochimica Acta Part A: Molecular and Biomolecular Spectroscopy.* 209 (2019) 95-99



Graphical abstract

**Highlights**

1. A lysosome-targeted fluorescence probe **NA-lyso** for monitoring HOBr was synthesized.
2. The probe can respond to HOBr with outstanding sensitivity and selectivity.
3. The probe can target in lysosome and monitoring the level of HOBr in Hela cells.
4. The probe can also be used to image HOBr in vivo.